



1 **Non biogenic source is an important but**  
2 **overlooked contributor to aerosol isoprene-**  
3 **derived organosulfates during winter in**  
4 **northern China**

5

6 Ting Yang<sup>1</sup>, Yu Xu<sup>1,2\*</sup>, Yu-Chen Wang<sup>3</sup>, Yi-Jia Ma<sup>1</sup>, Hong-Wei Xiao<sup>1,2</sup>, Hao Xiao<sup>1,2</sup>,  
7 Hua-Yun Xiao<sup>1,2</sup>

8

9 <sup>1</sup>School of Agriculture and Biology, Shanghai Jiao Tong University, Shanghai 200240,  
10 China

11 <sup>2</sup>Shanghai Yangtze River Delta Eco-Environmental Change and Management  
12 Observation and Research Station, Ministry of Science and Technology, Ministry of  
13 Education, Shanghai 200240, China

14 <sup>3</sup>Division of Environment and Sustainability, Hong Kong University of Science and  
15 Technology, Hong Kong SAR 00000, China

16

17

18

19

\*Corresponding authors

20

Yu Xu

21

E-mail: xuyu360@sjtu.edu.cn

22



23 **Abstract:** Previous measurement-model comparisons of atmospheric isoprene levels  
24 showed a significant unidentified source of isoprene in some northern Chinese cities  
25 during winter. Here, spatial variability in winter aerosol organosulfate (OS) formation  
26 in typical southern (Guangzhou and Kunming) and northern (Xi'an and Taiyuan)  
27 cities, China, was investigated to reveal the influence of potential non biogenic  
28 contributor on aerosol OS pollution levels. Monoterpene-derived OSs were  
29 significantly higher in southern cities than in northern cities, which was attributed to  
30 temperature dependent emission of monoterpenes (i.e., higher temperatures in  
31 southern cities drove more monoterpene emissions). However, isoprene-derived OSs  
32 (OS<sub>i</sub>) showed the opposite trend, with significantly higher levels in northern cities.  
33 Principal component analysis combined with field simulation combustion experiments  
34 suggested that biomass burning rather than gasoline, diesel, and coal combustion  
35 contributed significantly to the abundance of OS<sub>i</sub> in northern cities. The comparison  
36 of anthropogenic OS molecular characteristics between particles released from  
37 various combustion sources and ambient aerosol particles suggested that stronger  
38 biomass and fossil fuel combustion activities in northern cities promoted the  
39 formation of more anthropogenic OSs. Overall, this study provides direct molecular  
40 evidence for the first time that non biogenic sources can significantly contribute to the  
41 formation of OS<sub>i</sub> in China during winter.

42

43 **Keywords:** Aerosol organosulfates, Biogenic precursors, Anthropogenic precursors,  
44 Spatial variation, Influencing factors



## 45 **1. Introduction**

46 Organosulfates (OSs) with a sulfate ester functional group typically contribute 3–  
47 30% of the organic aerosol mass in atmospheric fine particles (PM<sub>2.5</sub>) (Luk'Ac's et al.  
48 2009). Moreover, OSs have been estimated to account for up to 12% of the total sulfur  
49 mass in fine particles, playing significant roles in the global biogeochemical cycling  
50 of sulfur (Luk'Ac's et al. 2009). In particular, OSs can impact the properties of  
51 aerosols, such as hygroscopicity, acidity, viscosity, and morphology, which are closely  
52 associated with the organic aerosol formation and urban air quality (Riva et al. 2019;  
53 Fleming et al. 2019). Thus, aerosol OSs have attracted significant attention over the  
54 years. However, the mechanisms and key factors impacting the formation and  
55 abundance of aerosol OSs in the real world remain considerable uncertainty, despite  
56 the important insights gained from laboratory simulation experiments (Wang et al.  
57 2021; Yang et al. 2023; Wang et al. 2020).

58 Previous field studies have indicated that acidity (Duporté et al. 2019), sulfate  
59 (Aoki et al. 2020), aerosol liquid water (Duporté et al. 2016), and oxidants (e.g.,  
60 ozone) (Wang et al. 2021) represent critical factors controlling the formation of OSs  
61 via heterogeneous and liquid phase processes (Brüggemann et al. 2020b). Precursor  
62 emission intensities (e.g., isoprene, monoterpenes, polycyclic aromatic hydrocarbons,  
63 and alkanes) also play an important role in impacting abundance of biogenic and  
64 anthropogenic OSs in ambient aerosols (Wang et al. 2022; Bryant et al. 2021; Yang et  
65 al. 2024). Furthermore, previous studies have identified a large number of CHOS  
66 compounds in smoke particles (e.g., pine branches, corn straw, rice straw, and coal)



67 (Song et al. 2019; Song et al. 2018; Tang et al. 2020). However, limited studies have  
68 focused on the contribution of different smoke particles to urban aerosol OSs. This  
69 may be an overlooked source of OSs. In general, few field studies have conducted a  
70 comprehensive investigation into the relationship between biogenic and  
71 anthropogenic impacting factors and regional differences in aerosol OS pollution.  
72 This hinders our understanding of the formation and constraints of aerosol OS  
73 pollution in a complex polluted atmospheric environment across diverse cities in  
74 China.

75 The considerable variations in climatic conditions and air pollution levels in the  
76 northern and southern regions of China during winter (Ding et al. 2014; Ding et al.  
77 2016b) provide a distinctive opportunity to examine the complex influences of  
78 precursors, humidity, acidity, atmospheric oxidants, and anthropogenic pollution on  
79 the formation and abundance of aerosol OSs in the real world (Yang et al. 2024; Yang  
80 et al. 2023; Wang et al. 2021; Hettiyadura et al. 2019). In this study, we conducted the  
81 simultaneous observations of OSs and other chemical components in PM<sub>2.5</sub> collected  
82 from typical southern (Guangzhou and Kunming) and northern (Xi'an and Taiyuan)  
83 cities in China during winter. Moreover, we also attempted to identify OSs in smoke  
84 particles emitted from combustion of different materials (i.e., rice straw, pine branch,  
85 diesel, gasoline, and coal). The principal aims of this study are 1) to investigate the  
86 spatial differences in aerosol OS pollution in northern and southern China during  
87 winter and 2) to elucidate the key factors that contribute to the spatial variability of  
88 OS pollution, with a focus on the OSs derived from smoke particles.



89 **2. Materials and Methods**

90 **2.1. Site description and sample collection**

91 The research sites are located in four urban areas in China, including Xi'an (XA)  
92 Taiyuan (TY), Guangzhou (GZ), and Kunming (KM) (**Figure S1a**). XA and TY are  
93 typical northern cities with cold winters (average temperature below 2 °C during the  
94 study period; **Table S1**). Thus, burning coal and biomass for heating is prevalent in  
95 these two cities during winter (Zhou et al. 2017; Ma et al. 2017), which significantly  
96 deteriorated the local air quality (**Figure S1b**). GZ and KM represent typical southern  
97 cities, with an average air temperature of over 10 °C during the winter sampling  
98 period (**Table S1**). Clearly, the distinctive climatic conditions in the northern and  
99 southern cities during winter may lead to significant spatial differences in the level of  
100 air pollution and the emission intensity of biogenic volatile organic compounds  
101 (VOCs) (Ding et al. 2014; Xu et al. 2024b).

102 From 10 December 2017 to 8 January 2018, sampling was performed  
103 simultaneously in four cities. Filters contained PM<sub>2.5</sub> were collected at regular two- to  
104 three-day intervals, with the collection duration being 24 hours, using a high-volume  
105 air sampler (Series 2031, Laoying, China) at a flow rate of ~1.05 m<sup>3</sup> min<sup>-1</sup> (Xu et al.  
106 2024a). A blank filter was sampled at each of the study sites. A total of four PM<sub>2.5</sub>  
107 samples were collected and stored at a temperature of -30°C. Meteorological data,  
108 including wind speed, relative humidity (RH), and temperature, were obtained from  
109 nearby environmental stations. Concurrently, the concentrations of various pollutants,  
110 such as O<sub>3</sub>, NO<sub>2</sub>, and SO<sub>2</sub>, were also recorded.



111 **2.2. Smoke particle collection**

112 The controlled burning experiments conducted in the field were designed to  
113 simulate the emissions of “real world” burning cases in China (**Figure S2**), with the  
114 methodology being improved according to the previous reports (He et al. 2010; Wang  
115 et al. 2017). Rice straw and pine branch are typical materials for biomass burning in  
116 China (Zhou et al. 2017). In addition, the combustion of coal, gasoline, and diesel was  
117 representative of fossil fuel combustion (Yu et al. 2020). Accordingly, the smoke  
118 particles (PM<sub>2.5</sub>) emitted from rice straw, pine branch, coal combustion, gasoline  
119 vehicle exhausts, and diesel vehicle exhausts were separately collected using self-  
120 made devices.

121 Briefly, the smoke from the combustion of rice straw, pine branch, and coal was  
122 sampled through a combustion furnace pumped with ambient air (particulate matter is  
123 removed) (**Figure S2a**). It should be noted that introducing ambient air with removed  
124 particulate matter into the combustion furnace is to minimize the pollution of ambient  
125 particulate matter to the smoke particle samples. This is the most distinct difference  
126 from the previous combustion experiment (Zhang et al. 2022; Xu et al. 2023a). Each  
127 combustion experiment for straw, pine branch, and coal lasted for 30–40 min.  
128 Regarding the smoke particles emitted from gasoline vehicle exhausts and diesel  
129 vehicle exhausts, they were collected for 3 hours by directly connecting to the car  
130 exhaust pipe (**Figure S2b**). All smoke particle samples are collected onto prebaked  
131 quartz fiber filters via a high-volume air sampler (Series 2031, Laoying, China). Four  
132 repeated experiments were conducted for each combustion material, one of which was



133 collected as a blank sample. All smoke particle samples were stored at  $-30^{\circ}\text{C}$ .

134

### 135 **2.3. Chemical analysis and predictions of aerosol acidity and water concentration**

136 The extraction, measurement procedures, and identification of OSs were  
137 described in detail in our recent publications (Yang et al. 2024). Briefly, the filter  
138 sample was extracted using methanol, then filtered through a  $0.22\ \mu\text{m}$  PTFE syringe  
139 filter and concentrated by a gentle stream of nitrogen gas. Subsequently, the  
140 concentrated sample with adding ultrapure water ( $300\ \mu\text{L}$ ) was thoroughly mixed  
141 using a mixer. The mixture was centrifuged to obtain the supernatant for analysis of  
142 UPLC-MS/MS system (Waters, USA) (Wang et al. 2021). The reverse-phase liquid  
143 chromatography (RPLC) method was used in this study. Although our method is quite  
144 effective in retaining and separating low molecular weight (MW) OSs, as  
145 demonstrated in our recent publication (Yang et al. 2024), we also acknowledge that  
146 the developed hydrophilic interaction liquid chromatography method may represent a  
147 optimized solution for the measurement of low-MW OSs (Cui et al. 2018; Hettiyadura  
148 et al. 2015).

149 In addition, it has been indicated in previous studies (Brüggemann et al. 2020a;  
150 Kristensen et al. 2016) that the levels of OSs can be affected by the sampling  
151 procedure, especially when  $\text{SO}_2$  removal procedures are not employed. On the  
152 assumption that  $\text{SO}_2$  reacts with organics on filters to form OSs, similar processes  
153 must also occur on ambient particles prior to sampling. Moreover, there is currently no  
154 study evaluating the relative efficiency of OS generation in filters and ambient



155 particles. Consequently, the possible consequences of sampling without denuding SO<sub>2</sub>  
156 for the quantification of OSs were not taken into account in our studies (Brüggemann  
157 et al. 2020a; Kristensen et al. 2016). In total, 212 OSs were identified. However, only  
158 111 OS species were quantified using surrogate standards in this study (**Table S2** and  
159 **S3**) (Wang et al. 2021; Hettiyadura et al. 2017). The study divided the several  
160 principal OS groups as follows: monoterpene-derived OSs (OS<sub>m</sub>), isoprene-derived  
161 OSs (OS<sub>i</sub>), C<sub>2</sub>–C<sub>3</sub> OSs (i.e., OSs with two or three carbon atoms), and anthropogenic  
162 OSs (i.e., aliphatic and aromatic OSs) (Yang et al. 2023). The specific classification  
163 and quantification methods were detailed in our recent publications (Yang et al. 2023;  
164 Yang et al. 2024) and **Supporting Information**.

165 An additional portion of each filter was extracted using ultrapure water for  
166 determining the inorganic ions (Huang et al. 2023). The concentrations of SO<sub>4</sub><sup>2-</sup>, Ca<sup>2+</sup>,  
167 NO<sub>3</sub><sup>-</sup>, Na<sup>+</sup>, K<sup>+</sup>, Mg<sup>2+</sup>, Cl<sup>-</sup>, and NH<sub>4</sub><sup>+</sup> were analyzed using ICS5000+ ion  
168 chromatography (Thermo, USA) (Yang et al. 2024). The mass concentration of  
169 aerosol liquid water (ALW) and pH value were calculated by a thermodynamic model  
170 (ISORROPIA-II) in the forward mode and thermodynamically metastable state, which  
171 was detailed in our previous studies (Liu et al. 2023; Lin et al. 2023; Xu et al. 2022;  
172 Xu et al. 2023b; Xu et al. 2020). The role of OSs in influencing ALW and pH was not  
173 included in this study because their impact on prediction outcomes was deemed to be  
174 insignificant.

175

176 **3. Results and Discussion**



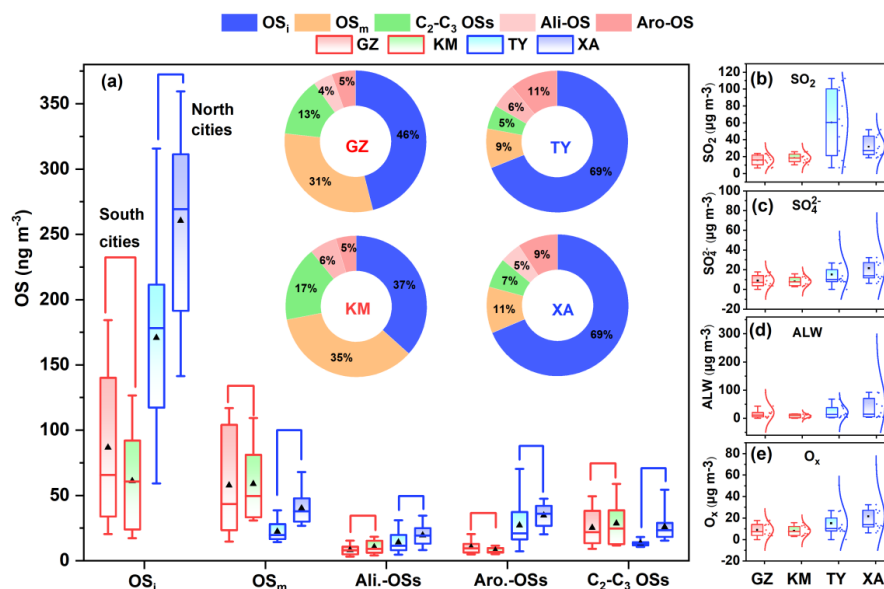


### 177 3.1. Spatial variations in concentrations and compositions of different OSs

178 **Figure 1a** shows the spatial distributions in mass concentrations and mass  
179 fractions of OS<sub>i</sub>, OS<sub>m</sub>, aliphatic OSs, aromatic OSs, and C<sub>2</sub>–C<sub>3</sub> OSs in PM<sub>2.5</sub> collected  
180 in southern (KM and GZ) and northern (TY and XA) cities during winter. On average,  
181 OS<sub>i</sub> was the dominant OS subgroup, which accounted for 37% – 46% and 68% – 69%  
182 of the total OS mass in southern and northern cities, respectively. The predominance  
183 of OS<sub>i</sub> in aerosol OSs was also reported by previous studies in cities in northern (e.g.,  
184 Beijing and Tianjin) (Wang et al. 2018; Ding et al. 2022) and southern (e.g.,  
185 Guangzhou and Shanghai) (Wang et al. 2022; Wang et al. 2021) China, as well as in  
186 coastal (the Yellow Sea and Bohai Sea) (Wang et al. 2023) and European (Sweden)  
187 (Kanellopoulos et al. 2022) and American regions (Chen et al. 2021; Hettiyadura et al.  
188 2017; Hettiyadura et al. 2019) (**Table S4**). Moreover, the concentrations of OS<sub>i</sub> were  
189 significantly lower in southern cities ( $61 \pm 38 \text{ ng m}^{-3} - 87 \pm 60 \text{ ng m}^{-3}$ ) than in  
190 northern cities ( $171 \pm 69 \text{ ng m}^{-3} - 260 \pm 71 \text{ ng m}^{-3}$ ) (**Table S1**), showing a  
191 concentration range overlapped with previous observations (**Table S4**). From southern  
192 to northern cities, the mass concentrations and mass fractions of OS<sub>m</sub> tended to  
193 decrease, which was opposite to the spatial variation pattern of OS<sub>i</sub> (**Figure 1a**). Both  
194 OS<sub>i</sub> and OS<sub>m</sub> are generally considered as typical biogenic OSs (Hettiyadura et al.  
195 2019; Wang et al. 2018), the abundances of which were tightly associated with  
196 biogenic VOC emissions when acidity, sulfate, atmospheric oxidation capacity, and  
197 ALW are not limiting factors (Bryant et al. 2021; Wang et al. 2022; Yang et al. 2024).  
198 Thus, these dissimilarities in the spatial variations of OS<sub>i</sub> and OS<sub>m</sub> can be attributed to



199 large differences in the intensity of biogenic VOC emissions (Wang et al. 2022)  
 200 and/or the key factors that constrain OS formation between the northern and southern  
 201 regions of China (**Table S1**).



202  
 203 **Figure 1** Box and whisker plots showing the variations in the concentration of  
 204 different OS groups in PM<sub>2.5</sub> collected in southern (GZ and KM) and northern (TY  
 205 and XA) cities of China during winter. Each box encompasses the 25th–75th  
 206 percentiles. Whiskers are the minimum and maximum values. The triangles and solid  
 207 lines inside boxes indicate the mean and median. The spatial variation in average  
 208 percentage distributions of various OS groups was shown in panel (a). Spatial  
 209 variations in (b) SO<sub>2</sub>, (c) SO<sub>4</sub><sup>2-</sup>, (d) ALW, and (e) O<sub>x</sub> levels.

210

211 The abundance of anthropogenic OSs (i.e., OS<sub>a</sub>, including aliphatic and aromatic  
 212 OSs) in southern cities was lower than that of OS<sub>m</sub>, which was opposite to the case in



213 the northern cities showing higher anthropogenic OS abundance (**Figure 1a** and  
214 **Table S1**). Moreover, we found that the spatial variation patterns of OS<sub>i</sub> and OS<sub>a</sub> were  
215 similar to those of SO<sub>2</sub>, SO<sub>4</sub><sup>2-</sup>, ALW, and O<sub>x</sub> (**Figures 1b–e**), as indicated by significant  
216 ( $P < 0.05$ ) correlations of OS<sub>i</sub> and OS<sub>a</sub> with those factors (**Figure S3**). However, OS<sub>m</sub>  
217 and C<sub>2</sub>–C<sub>3</sub> OSs showed an opposite spatial variation pattern to SO<sub>2</sub>, SO<sub>4</sub><sup>2-</sup>, ALW, and  
218 O<sub>x</sub> (**Figure 1**). If both OS<sub>i</sub> and OS<sub>m</sub> are assumed to be formed mainly from the  
219 oxidation of biologically emitted VOCs, the higher SO<sub>2</sub>, SO<sub>4</sub><sup>2-</sup>, ALW, and O<sub>x</sub> levels  
220 could theoretically lead to higher OS<sub>m</sub> in northern cities, just as these factors led to  
221 higher OS<sub>i</sub> abundance in northern cities (**Figure 1** and **Figure S3**). Accordingly, the  
222 above differentiated spatial variation patterns among different OS subgroups likely  
223 indicated that other sources of isoprene contributed to the formation of OS<sub>i</sub> in  
224 northern cities. Given the significant ( $P < 0.05$ ) correlations between OS<sub>i</sub> and OS<sub>a</sub>  
225 (**Figure S3**), non biogenic isoprene emissions may play an important role in the  
226 formation of aerosol OS<sub>i</sub> in northern cities. This will be further demonstrated in the  
227 following discussion.

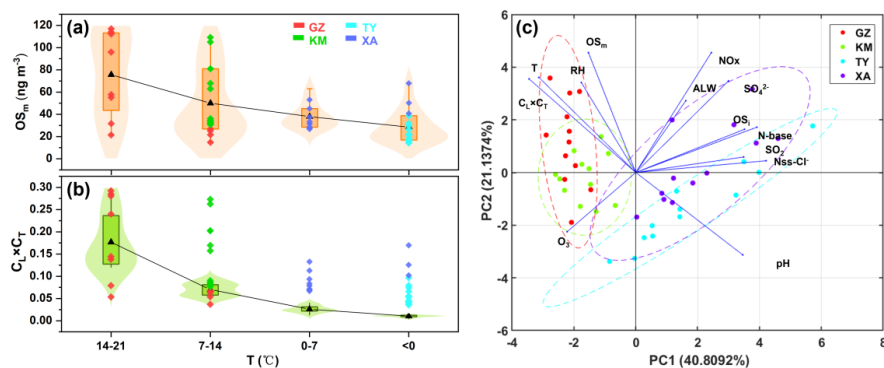
228

### 229 **3.2. Key factors affecting spatial differences in monoterpene-derived OS** 230 **abundance**

231 **Figure 2a** shows the distribution of OS<sub>m</sub> concentration as a function of air  
232 temperature. We found that the OS<sub>m</sub> concentration tended to increase with the increase  
233 of air temperature. Specifically, the air temperature in the southern cities was mainly  
234 in the range of 7–14°C during the sampling period, corresponding to higher aerosol



235 OS<sub>m</sub> abundance. In contrast, the low temperature (< 7°C) in the northern cities  
236 corresponded to a significant decrease in OS<sub>m</sub> abundance. This finding was similar to  
237 the previously observed decrease in aerosol OS<sub>m</sub> compounds with decreasing  
238 temperature during winter in Guangzhou (Bryant et al. 2021). Furthermore, the  
239 indicator ( $C_L \times C_T$ ) of biogenic VOC emission rate was also higher in southern cities  
240 than in northern cities (**Figure 2b**), which implied higher monoterpene emissions in  
241 southern cities. It has been suggested that the emission rates of biogenic VOCs (e.g.,  
242 monoterpene and isoprene) can be driven by increased air temperature and lighting  
243 (Ding et al. 2016a; Ding et al. 2016b). A previous study also found that the  
244 concentrations of atmospheric monoterpenes during the winter season were higher in  
245 warmer southern Chinese cities than in colder northern Chinese cities (Ding et al.  
246 2016b; Li et al. 2020). In particular, GZ and KM, which encompass extensive areas of  
247 coniferous and broad-leaved forests, have been identified as hotspots for monoterpene  
248 and isoprene emissions (Li and Xie 2014). Considering the lower levels of key  
249 factors affecting OS formation observed in southern cities (**Figures 1b–e** and **Table**  
250 **S1**), it can be inferred that the significant spatial differences in OS<sub>m</sub> abundances were  
251 largely attributed to temperature dependent emission of monoterpenes.



252

253 **Figure 2** Distribution of (a)  $OS_m$  and (b)  $C_L \times C_T$  data in different temperature ranges

254 during winter. The triangles inside boxes indicate the mean. Principal component

255 analysis result (c) deciphering the relationship among  $OS_i$ ,  $OS_m$ , and key factors

256 influencing  $OS$  formation.

257

258 To further determine the key factors affecting the spatial differences of  $OS_m$ ,

259 principal component analysis was conducted (**Figure 2c**). It can be easily determined

260 that the abundance of aerosol  $OS_m$  was closely related to changes in air temperature

261 and  $C_L \times C_T$  value. This precisely explained the changes in  $OS_m$  data in the southern

262 cities. In contrast, the abundance of aerosol  $OS_i$  in the northern cities was more

263 influenced by anthropogenic factors, as indicated by combustion source tracers such

264 as nitrogen-containing bases (N-bases) and non-sea-salt  $Cl^-$  ( $nss-Cl^-$ ) (Wang et al.

265 2017; Jiang et al. 2023) (**Figure 2c**). Thus, principal component analysis can perfectly

266 distinguish the main factors causing changes in  $OS_m$  and  $OS_i$  abundances between the

267 northern and southern cities. In general, the above results confirm that the spatial

268 variation of  $OS_m$  was predominantly controlled by temperature-related monoterpene



269 emissions. However, this cannot fully account for the observed spatial variation of  
270 OS<sub>i</sub>. Interestingly, the spatial distribution patterns of OS<sub>m</sub> and OS<sub>i</sub> in northern and  
271 southern China exhibited consistency during summer, closely resembling the spatial  
272 distribution of biogenic VOC emission intensities (Wang et al. 2022). Thus, this case  
273 together with our observations during winter further imply that non biogenic sources  
274 of isoprene were important contributors to the formation of OS<sub>i</sub> in northern China  
275 during winter.

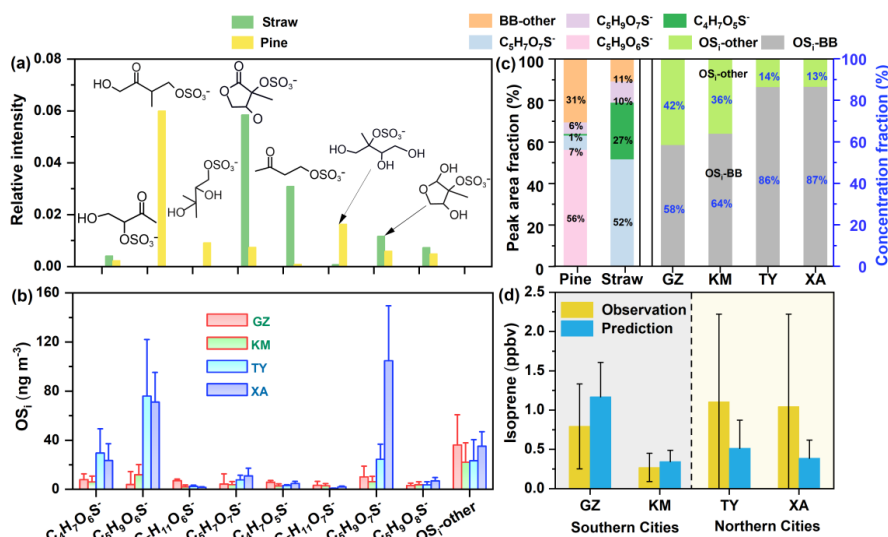
276

### 277 **3.3. Significant contribution of biomass burning to isoprene-derived OSs in** 278 **Northern China**

279 The previous principal component analysis has suggested that the abundance of  
280 OS<sub>i</sub> in northern cities was closely related to the levels of combustion source tracers  
281 (e.g., N-base compounds and nss-Cl<sup>-</sup>). To further confirm the potential contribution of  
282 combustion release to aerosol OS<sub>i</sub>, OSs in smoke particles (PM<sub>2.5</sub>) emitted from rice  
283 straw, pine branch, and coal combustion, as well as from gasoline vehicle exhausts,  
284 and diesel vehicle exhausts, were investigated. A total of 8 distinct OS<sub>i</sub> were identified  
285 in both the smoke particles emitted from biomass burning (rice straw and pine branch)  
286 and the ambient aerosol particles, including C<sub>4</sub>H<sub>7</sub>O<sub>6</sub>S<sup>-</sup>, C<sub>5</sub>H<sub>9</sub>O<sub>6</sub>S<sup>-</sup>, C<sub>5</sub>H<sub>11</sub>O<sub>6</sub>S<sup>-</sup>,  
287 C<sub>5</sub>H<sub>7</sub>O<sub>7</sub>S<sup>-</sup>, C<sub>4</sub>H<sub>7</sub>O<sub>5</sub>S<sup>-</sup>, C<sub>3</sub>H<sub>11</sub>O<sub>7</sub>S<sup>-</sup>, C<sub>5</sub>H<sub>9</sub>O<sub>7</sub>S<sup>-</sup>, and C<sub>5</sub>H<sub>9</sub>O<sub>8</sub>S<sup>-</sup>. Moreover, the peak  
288 intensities of these 8 OS<sub>i</sub> in smoke particles emitted from fossil fuel combustion  
289 (gasoline and diesel vehicle exhausts and coal) were close to those in the blank  
290 sample. A previous investigation into CHOS compounds in smoke particles emitted



291 from residential coal combustion and biomass burning also failed to identify OS<sub>i</sub>  
292 species (Song et al. 2019; Song et al. 2018), which further supported the reliability of  
293 the combustion experiment conducted in this study. C<sub>5</sub>H<sub>9</sub>O<sub>6</sub>S<sup>-</sup> was dominant OS<sub>i</sub>  
294 species in pine-derived smoke particles (**Figure 3a,c**). We found that the average  
295 concentration of C<sub>5</sub>H<sub>9</sub>O<sub>6</sub>S<sup>-</sup> in ambient aerosol samples was much higher in northern  
296 cities than in southern cities (**Figure 3b**). A reasonable explanation for this is that pine  
297 branches are commonly used as solid fuel for heating and cooking in northern suburbs  
298 and rural areas (Zhou et al. 2017). C<sub>5</sub>H<sub>7</sub>O<sub>7</sub>S<sup>-</sup> and C<sub>4</sub>H<sub>7</sub>O<sub>5</sub>S<sup>-</sup> dominated OS<sub>i</sub> species in  
299 straw-derived smoke particles (**Figure 3a,c**). However, these two types of OS<sub>i</sub> have  
300 relatively low abundance in ambient aerosol samples in both northern and southern  
301 cities. This may be attributed to the fact that straw burning was mainly concentrated  
302 in autumn rather than winter in China (Zhou et al. 2017; Yang et al. 2015). On  
303 average, the biomass burning-related OS<sub>i</sub> accounted for 58% – 64% and 86% – 87%  
304 of the total OS<sub>i</sub> concentration in southern and northern cities, respectively (**Figure 3c**).  
305 Although these biomass burning-related OS<sub>i</sub> can also be formed through atmospheric  
306 transformation of biogenic isoprene, the higher proportion of these OS<sub>i</sub> in northern  
307 cities together with previous principal component analysis results still support our  
308 previous consideration that non biogenic OS<sub>i</sub> may be an important contributor to  
309 aerosol OS<sub>i</sub> in northern cities.



310

311 **Figure 3** Relative signal intensity of (a) identified major OS<sub>i</sub> species in different types  
 312 of smoke particle samples. Spatial variation in the concentration of OS<sub>i</sub> identified in  
 313 smoke particles in (b) ambient PM<sub>2.5</sub> samples. Peak area and concentration fraction of  
 314 (c) OS<sub>i</sub> species identified in both ambient PM<sub>2.5</sub> samples collected in different cities  
 315 and smoke particles. Comparison of (d) isoprene mixing ratios obtained from  
 316 observation and modeling in different cities (Zhang et al. 2020).

317

318 Previous laboratory studies have suggested that these identified OS<sub>i</sub> species in  
 319 biomass burning-derived smoke particles are typically formed through heterogeneous  
 320 and multiphase reactions associated with isoprene, its oxidation intermediates, and  
 321 sulfate or sulfur dioxide (Surratt et al. 2008; Surratt et al. 2007; Darer et al. 2011).  
 322 Specifically, C<sub>5</sub>H<sub>9</sub>O<sub>6</sub>S<sup>-</sup>, as a sulfate ester of C<sub>5</sub>-alkene triols, was formed mainly  
 323 through the uptake of gas-phase isoprene oxidation products onto acidified sulfate  
 324 aerosol (Surratt et al. 2007). The formation of C<sub>5</sub>H<sub>7</sub>O<sub>7</sub>S<sup>-</sup> and C<sub>5</sub>H<sub>9</sub>O<sub>7</sub>S<sup>-</sup> begins with





325 the gas-phase oxidation of isoprene (Surratt et al. 2008).  $C_4H_7O_6S^-$  can be generated  
326 both from isoprene photooxidation and sulfate radical reaction with methacrolein  
327 (MACR) or methyl vinyl ketone (MVK) (Schindelka et al. 2013; Wach et al. 2019;  
328 Nozière et al. 2010).  $C_5H_{11}O_7S^-$  was produced by reactive uptake of isoprene-derived  
329 epoxide (IEPOX) on sulfate under low-NO<sub>x</sub> conditions. Since our combustion  
330 experiments have excluded the direct contribution of ambient aerosol particles to OS<sub>i</sub>  
331 in smoke particles, it can be expected that these detected OS<sub>i</sub> compounds were mainly  
332 generated within smoke plumes through the isoprene oxidation pathway mentioned  
333 above. It has been demonstrated that directly emitted organic aerosols or VOCs can  
334 undergo a chemical reaction within smoke plumes, forming secondary organic  
335 compounds within a matter of hours (Wang et al. 2017; Song et al. 2018; Mason et al.  
336 2001). A field study conducted by Zhu et al. (2016) at a rural site (Yucheng) in the  
337 North China Plain (NCP) region has observed that the concentration of ambient  
338 isoprene during the period of straw combustion was approximately twice as high as  
339 that observed during periods of non combustion. In addition, Li et al. (2018) found  
340 that isoprene-derived epoxides increased significantly during field open burning of  
341 straw. Generally, despite the fact that a few of the mechanisms by which OSs are  
342 formed have been verified through field studies, the formation of CHOS and CHONS  
343 compounds has been observed to occur in the biomass burning plume (Zhang et al.  
344 2024; Song et al. 2018; Tang et al. 2020). Thus, these previous case studies further  
345 support our consideration that OS<sub>i</sub> compounds formed in biomass burning-derived  
346 smoke particles in this study can be attributed to increasing isoprene emission caused



347 by field biomass burning (Zhu et al. 2016) and favorable aqueous secondary organic  
348 aerosols (SOA) formation during the aging process of the biomass burning plume  
349 (Gilardoni et al. 2016).

350 **Figure 3d** presents a comparison between the isoprene mixing ratios derived  
351 from model simulations (plant functional type related model) and those observed in  
352 the field in different Chinese cities during winter (December and January) (Zhang et  
353 al. 2020). Overall, the levels of isoprene observed in northern cities during winter  
354 were higher than those in southern cities. In addition, the predicted values in southern  
355 cities were slightly higher than the observed values, which may be attributed to the  
356 lag in model prediction results caused by the rapid urbanization rates in these southern  
357 cities (Zhang et al. 2020). However, the observed values in these two northern cities  
358 were 53% to 63% higher than the predicted values, on average. Clearly, this plant  
359 functional type related isoprene prediction model cannot explain the large amount of  
360 “missing” isoprene sources in northern cities. Thus, the observed spatial differences in  
361  $OS_i$  (**Figure 1**) and field combustion experiments (**Figure 3**) can suggest that these  
362 “missing” isoprene sources were mainly derived from biomass burning, significantly  
363 contributing to the production of aerosol  $OS_i$  in northern cities. This can be also  
364 supported by previous principal component analysis and correlation analysis among  
365 combustion source tracers and  $OS_i$  species (**Figure 2** and **Figure S4**).

366

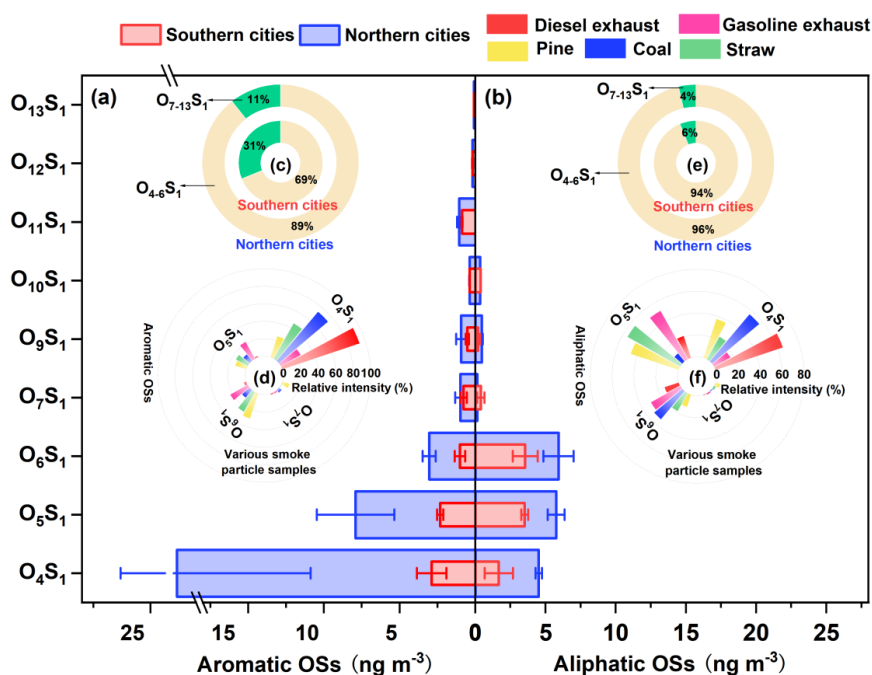
367 **3.4. Formation of anthropogenic OSs mainly driven by fossil fuel and biomass**  
368 **combustion**



369           **Figures 4a,b** show the average concentration distribution of anthropogenic OSs  
370 classified based on the number of O atoms in their molecules in southern (GZ and  
371 KM) and northern (TY and XA) cities. The O<sub>4</sub>S<sub>1</sub> subgroup was the most abundant  
372 aromatic OSs in both southern and northern cities, among which C<sub>9</sub>H<sub>9</sub>O<sub>4</sub>S<sup>-</sup>, phenyl  
373 sulfate (C<sub>6</sub>H<sub>5</sub>O<sub>4</sub>S<sup>-</sup>), and benzyl sulfate (C<sub>7</sub>H<sub>7</sub>O<sub>4</sub>S<sup>-</sup>) were dominant species (**Table S3**).  
374 C<sub>7</sub>H<sub>7</sub>O<sub>4</sub>S<sup>-</sup> and C<sub>6</sub>H<sub>5</sub>O<sub>4</sub>S<sup>-</sup> have been suggested to be formed mainly through the  
375 photooxidation of 2-methylnaphthalene and naphthalene (Riva et al. 2015), or  
376 alternatively, by the sulfate radical reaction with aromatic compounds, including  
377 toluene and benzoic acid, in an aqueous phase environment (Riva et al. 2015). The  
378 formation mechanism of C<sub>9</sub>H<sub>9</sub>O<sub>4</sub>S<sup>-</sup> is rarely reported. However, C<sub>9</sub>H<sub>9</sub>O<sub>4</sub>S<sup>-</sup>, C<sub>6</sub>H<sub>5</sub>O<sub>4</sub>S<sup>-</sup>,  
379 and C<sub>7</sub>H<sub>7</sub>O<sub>4</sub>S<sup>-</sup> were also detected in both fossil fuel combustion-derived smoke  
380 particles and biomass burning-derived smoke particles (**Figure S5** and **Table S5**),  
381 indicating that the aromatic VOCs produced by fuel combustion are closely related to  
382 the formation of these aromatic OSs. Overall, aerosol aromatic OS compounds in both  
383 southern and northern cities were mainly distributed between four and six O atoms  
384 (**Figure 4c**), which was similar to the distribution of aromatic OSs identified in  
385 various smoke particles emitted from different combustion sources (**Figure 4d**).  
386 However, the average abundances of aromatic O<sub>4-6</sub>S<sub>1</sub> compounds in northern cities  
387 were 3–6 times higher than those in southern cities. The above results suggest that  
388 aromatic OSs originated from fossil fuel and biomass combustion activities are  
389 important contributors to urban aerosol anthropogenic OSs in winter in China,  
390 especially in northern cities. We found that the correlations between aromatic OSs and



391 anthropogenic indicators ( $\text{SO}_2$ ,  $\text{SO}_4^{2-}$ , N-base, and nss- $\text{Cl}^-$ ) were stronger in northern  
 392 cities than in southern cities (**Figure S6**), and that the release of polycyclic aromatic  
 393 hydrocarbons from fossil fuel combustion was also higher in northern cities (**Figure**  
 394 **S7**). This further indicates that higher aerosol aromatic OSs in northern cities was  
 395 mainly attributed to stronger combustion activities in those cities.



396  
 397 **Figure 4** Concentration distribution of different (a) aromatic and (b) aliphatic OS  
 398 subgroups (classification based on oxygen atoms) in southern and northern cities.  
 399 Ring charts (c,e) show the percentage contributions of O<sub>4-6</sub>S<sub>1</sub> and O<sub>7-13</sub>S<sub>1</sub> subgroups.  
 400 Radial bar charts (d,f) illustrate the relative signal intensity of different OS subgroups  
 401 in different smoke particle samples.

402

403 Aliphatic OSs were also predominantly distributed between O<sub>4</sub>S<sub>1</sub> and O<sub>6</sub>S<sub>1</sub>



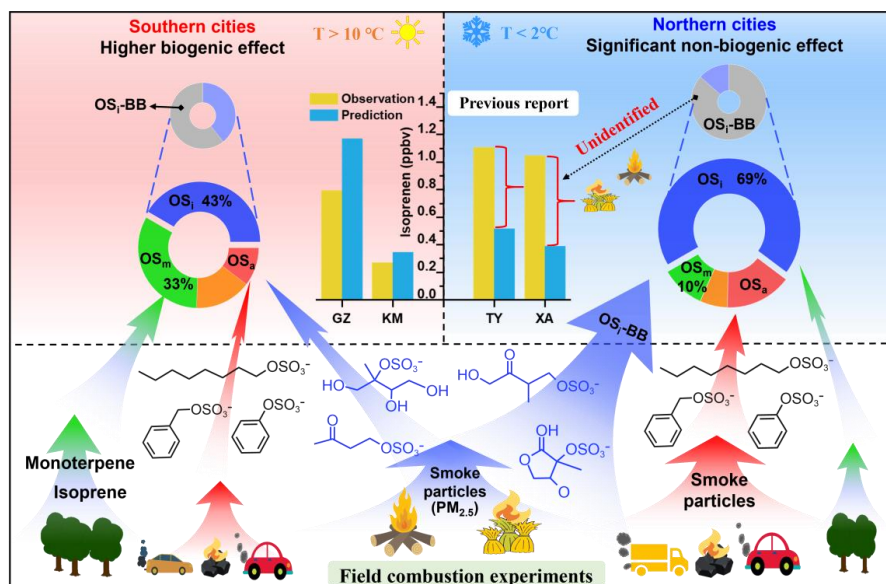
404 subgroups in both southern and northern cities (**Figures 4b,e**), which was similar to  
405 the case found in both fossil fuel combustion-derived smoke particles and biomass  
406 burning-derived smoke particles (**Figure 4f**). It has been suggested that the long-chain  
407 alkanes derived from traffic emissions can largely contribute to the formation of  
408 CHOS compounds with aliphatic carbon chains (Tao et al. 2014). In addition, Tang et  
409 al. (2020) analyzed the molecular compositions of smoke particles from open biomass  
410 burning, household coal combustion and vehicle emissions and suggested that the  
411 aliphatic CHOS compounds can be derived from both vehicle emissions and coal and  
412 biomass combustion. In this study, aliphatic OSs showed a significant ( $P < 0.05$ )  
413 positive correlation with  $\text{nss-Cl}^-$ ,  $\text{SO}_2$ ,  $\text{NO}_x$ , and N-base compounds in both southern  
414 and northern cities (**Figure S8**), indicating aerosol aliphatic OSs were affected by a  
415 combination of biomass burning and vehicle emissions in those cities during winter.  
416 Thus, the significantly higher level of aliphatic  $\text{O}_{4-6}\text{S}_1$  species in northern cities  
417 indicated that the formation of aliphatic OSs in northern cities was more driven by  
418 pollutants released from the combustion of fossil fuels and biomass compared to  
419 southern cities. This consideration is highly consistent with the fact that the  
420 concentrations of air pollutants (e.g.,  $\text{SO}_2$  and  $\text{NO}_2$ ) in northern cities with a large  
421 demand for heating during winter are usually higher than those in warmer southern  
422 cities (**Figure S1b**) (Yu et al. 2020; Ding et al. 2017; Ma et al. 2017; Zhou et al.  
423 2017).

424

425 **4. Conclusion and atmospheric implications**



426 It has been previously suggested that isoprene can also be released into the  
427 atmosphere as a result of open burning of agricultural residues and forest fires  
428 (Andreae 2019; Simpson et al. 2011). A field study conducted by Wang et al. (2019)  
429 in Beijing during winter inferred that the prevalence of OS<sub>i</sub> compounds in total  
430 aerosol OSs may be partially attributable to biomass burning emissions, although  
431 there was a paucity of compelling evidence to support this hypothesis. This work  
432 combines strongly contrasting observational studies (northern Chinese Cities vs  
433 southern Chinese Cities) with in situ combustion modelling experiments to provide  
434 the first direct evidence that biomass burning emission, rather than fossil fuel  
435 combustion emission, is a significant contributor to aerosol OS<sub>i</sub> in northern cities  
436 (**Figure 5**). In Chinese cities, particularly those in the northern region, biomass  
437 materials are extensively utilized for domestic heating and cooking purposes during  
438 the winter season (Zhou et al. 2017). Clearly, the isoprene emissions from biomass  
439 combustion sources would result in higher isoprene mixing ratios than those  
440 simulated by the model (Zhang et al. 2020) that only considers natural isoprene  
441 emissions. Thus, isoprene prediction models applied to Chinese winters in the future  
442 should also take into account the various biomass combustion source releases.  
443 Furthermore, biogenic OSs are important SOA constituents and have been frequently  
444 serve as important tracers for biogenic SOA (Ding et al. 2014; Ding et al. 2016a). The  
445 overall results suggest that some OS<sub>i</sub> species may not be suitable as biogenic SOA  
446 markers, especially in areas with intensive biomass burning activities, such as  
447 northern Chinese cities during winter.



448

449 **Figure 5** Conceptual picture showing the characteristics and main contributors of OS  
450 in northern and southern China during winter.

451

452 We found that different fossil fuel combustion emissions (e.g., vehicle emissions  
453 and coal combustion emissions) and biomass burning emissions can contribute to  
454 aerosol anthropogenic OSs. However, current studies have not been able to accurately  
455 distinguish between the contributions of various material combustion to different  
456 types of anthropogenic OSs. Future research is necessary to develop more  
457 comprehensive models to further explore the effects of various combustion sources on  
458 the generation and reduction of urban aerosol OS pollution. Of particular importance  
459 is that although the production of various OSs was directly observed through our  
460 simulated combustion experiments, it is not clear whether the chemical mechanisms  
461 involved are similar to those derived from the laboratory simulations. This is because



462 the combustion process is accompanied by the effects of high temperatures. In  
463 general, although our results provide direct evidence for the release of OSs from  
464 combustion of various combustion sources, further mechanistic studies and  
465 environmental impact assessment are still urgently needed. This may be important for  
466 effective control of urban wintertime organic aerosol pollution in China.

467

#### 468 **Data availability**

469 The data presented in this work are available upon request from the corresponding  
470 authors.

471

#### 472 **Competing interests**

473 The authors declare no conflicts of interest relevant to this study.

474

#### 475 **Supplement**

476 Additional information regarding descriptions of classification of OSs (Text S1 and  
477 Table S2–S3), quantification of OSs (Text S2), estimating of isoprene emission rate  
478 (Text S3), the OS concentrations showed in previous studies (Table S4), the location  
479 of the sampling site (Figure S1), smoke particle collection (Figure S2), and more data  
480 (Table S1, Table S5, and Figures S3–S8).

481

#### 482 **Author contributions**

483 YX designed the study. TY, YJM, HWX, and HX performed field measurements and





484 sample collection; TY and YJM performed chemical analysis; YX and TY performed  
485 data analysis; YX and TY wrote the original manuscript; and YX, TY, YCW, and  
486 HXX reviewed and edited the manuscript.

487

#### 488 **Acknowledgements**

489 The authors are very grateful to Jian-Zhen Yu at the Hong Kong University of Science  
490 and Technology for her kind and valuable comments to improve the paper.

491

#### 492 **Financial support**

493 This study was kindly supported by the National Natural Science Foundation of China  
494 (grant number 42303081 and 22306059), the Shanghai “Science and Technology  
495 Innovation Action Plan” Shanghai Sailing Program (grant number 22YF1418700),  
496 and the National Key Research and Development Program of China (grant number  
497 2023YFF0806001).

498

499

500



501 **References**

502 Andreae, M. O.: Emission of trace gases and aerosols from biomass burning – an  
503 updated assessment, *Atmos. Chem. Phys.*, 19, 8523-8546, 10.5194/acp-19-8523-  
504 2019, 2019.

505 Aoki, E., Sarrimanolis, J. N., Lyon, S. A., and Elrod, M. J.: Determining the Relative  
506 Reactivity of Sulfate, Bisulfate, and Organosulfates with Epoxides on Secondary  
507 Organic Aerosol, *ACS Earth and Space Chemistry*, 4, 1793-1801,  
508 10.1021/acsearthspacechem.0c00178, 2020.

509 Brüggemann, M., Riva, M., Perrier, S., Poulain, L., George, C., and Herrmann, H.:  
510 Overestimation of Monoterpene Organosulfate Abundance in Aerosol Particles  
511 by Sampling in the Presence of SO<sub>2</sub>, *Environmental Science & Technology*  
512 *Letters*, 8, 206-211, 10.1021/acs.estlett.0c00814, 2020a.

513 Brüggemann, M., Xu, R., Tilgner, A., Kwong, K. C., Mutzel, A., Poon, H. Y., Otto, T.,  
514 Schaefer, T., Poulain, L., Chan, M. N., and Herrmann, H.: Organosulfates in  
515 Ambient Aerosol: State of Knowledge and Future Research Directions on  
516 Formation, Abundance, Fate, and Importance, *Environ. Sci. Technol.*, 54, 3767-  
517 3782, 10.1021/acs.est.9b06751, 2020b.

518 Bryant, D. J., Elzein, A., Newland, M., White, E., Swift, S., Watkins, A., Deng, W.,  
519 Song, W., Wang, S., Zhang, Y., Wang, X., Rickard, A. R., and Hamilton, J. F.:  
520 Importance of Oxidants and Temperature in the Formation of Biogenic  
521 Organosulfates and Nitrooxy Organosulfates, *ACS Earth and Space Chemistry*,  
522 5, 2291-2306, 10.1021/acsearthspacechem.1c00204, 2021.



- 523 Chen, Y., Dombek, T., Hand, J., Zhang, Z., Gold, A., Ault, A. P., Levine, K. E., and  
524 Surratt, J. D.: Seasonal Contribution of Isoprene-Derived Organosulfates to Total  
525 Water-Soluble Fine Particulate Organic Sulfur in the United States, *ACS Earth  
526 and Space Chemistry*, 5, 2419-2432, 10.1021/acsearthspacechem.1c00102, 2021.
- 527 Cui, T., Zeng, Z., dos Santos, E. O., Zhang, Z., Chen, Y., Zhang, Y., Rose, C. A.,  
528 Budisulistiorini, S. H., Collins, L. B., Bodnar, W. M., de Souza, R. A. F., Martin,  
529 S. T., Machado, C. M. D., Turpin, B. J., Gold, A., Ault, A. P., and Surratt, J. D.:  
530 Development of a hydrophilic interaction liquid chromatography (HILIC)  
531 method for the chemical characterization of water-soluble isoprene epoxydiol  
532 (IEPOX)-derived secondary organic aerosol, *Environmental Science: Processes  
533 & Impacts*, 20, 1524-1536, 10.1039/c8em00308d, 2018.
- 534 Darer, A. I., Cole-Filipiak, N. C., O'Connor, A. E., and Elrod, M. J.: Formation and  
535 Stability of Atmospherically Relevant Isoprene-Derived Organosulfates and  
536 Organonitrates, *Environ. Sci. Technol.*, 45, 1895-1902, 10.1021/es103797z,  
537 2011.
- 538 Ding, S., Chen, Y., Devineni, S. R., Pavuluri, C. M., and Li, X.-D.: Distribution  
539 characteristics of organosulfates (OSs) in PM<sub>2.5</sub> in Tianjin, Northern China:  
540 Quantitative analysis of total and three OS species, *Sci. Total Environ.*, 834,  
541 10.1016/j.scitotenv.2022.155314, 2022.
- 542 Ding, X., He, Q.-F., Shen, R.-Q., Yu, Q.-Q., and Wang, X.-M.: Spatial distributions of  
543 secondary organic aerosols from isoprene, monoterpenes,  $\beta$ -caryophyllene, and  
544 aromatics over China during summer, *J. Geophys. Res. Atmos.*, 119, 11,877-



- 545 811,891, 10.1002/2014jd021748, 2014.
- 546 Ding, X., He, Q.-F., Shen, R.-Q., Yu, Q.-Q., Zhang, Y.-Q., Xin, J.-Y., Wen, T.-X., and  
547 Wang, X.-M.: Spatial and seasonal variations of isoprene secondary organic  
548 aerosol in China: Significant impact of biomass burning during winter, Scientific  
549 Reports, 6, 10.1038/srep20411, 2016a.
- 550 Ding, X., Zhang, Y.-Q., He, Q.-F., Yu, Q.-Q., Wang, J.-Q., Shen, R.-Q., Song, W.,  
551 Wang, Y.-S., and Wang, X.-M.: Significant Increase of Aromatics-Derived  
552 Secondary Organic Aerosol during Fall to Winter in China, Environ. Sci.  
553 Technol., 51, 7432-7441, 10.1021/acs.est.6b06408, 2017.
- 554 Ding, X., Zhang, Y. Q., He, Q. F., Yu, Q. Q., Shen, R. Q., Zhang, Y., Zhang, Z., Lyu,  
555 S. J., Hu, Q. H., Wang, Y. S., Li, L. F., Song, W., and Wang, X. M.: Spatial and  
556 seasonal variations of secondary organic aerosol from terpenoids over China, J.  
557 Geophys. Res.Atmos., 121, 10.1002/2016jd025467, 2016b.
- 558 Duporté, G., Flaud, P. M., Geneste, E., Augagneur, S., Pangui, E., Lamkaddam, H.,  
559 Gratien, A., Doussin, J. F., Budzinski, H., Villenave, E., and Perraudin, E.:  
560 Experimental Study of the Formation of Organosulfates from  $\alpha$ -Pinene  
561 Oxidation. Part I: Product Identification, Formation Mechanisms and Effect of  
562 Relative Humidity, The Journal of Physical Chemistry A, 120, 7909-7923,  
563 10.1021/acs.jpca.6b08504, 2016.
- 564 Duporté, G., Flaud, P. M., Kammer, J., Geneste, E., Augagneur, S., Pangui, E.,  
565 Lamkaddam, H., Gratien, A., Doussin, J. F., Budzinski, H., Villenave, E., and  
566 Perraudin, E.: Experimental Study of the Formation of Organosulfates from  $\alpha$ -



- 567 Pinene Oxidation. 2. Time Evolution and Effect of Particle Acidity, *The Journal*  
568 *of Physical Chemistry A*, 124, 409-421, 10.1021/acs.jpca.9b07156, 2019.
- 569 Fleming, L. T., Ali, N. N., Blair, S. L., Roveretto, M., George, C., and Nizkorodov, S.  
570 A.: Formation of Light-Absorbing Organosulfates during Evaporation of  
571 Secondary Organic Material Extracts in the Presence of Sulfuric Acid, *ACS*  
572 *Earth and Space Chemistry*, 3, 947-957, 10.1021/acsearthspacechem.9b00036,  
573 2019.
- 574 Gilardoni, S., Massoli, P., Paglione, M., Giulianelli, L., Carbone, C., Rinaldi, M.,  
575 Decesari, S., Sandrini, S., Costabile, F., Gobbi, G. P., Pietrogrande, M. C.,  
576 Visentin, M., Scotto, F., Fuzzi, S., and Facchini, M. C.: Direct observation of  
577 aqueous secondary organic aerosol from biomass-burning emissions,  
578 *Proceedings of the National Academy of Sciences*, 113, 10013-10018,  
579 10.1073/pnas.1602212113, 2016.
- 580 He, L. Y., Lin, Y., Huang, X. F., Guo, S., Xue, L., Su, Q., Hu, M., Luan, S. J., and  
581 Zhang, Y. H.: Characterization of high-resolution aerosol mass spectra of  
582 primary organic aerosol emissions from Chinese cooking and biomass burning,  
583 *Atmos. Chem. Phys.*, 10, 11535-11543, 10.5194/acp-10-11535-2010, 2010.
- 584 Hettiyadura, A. P. S., Al-Naiema, I. M., Hughes, D. D., Fang, T., and Stone, E. A.:  
585 Organosulfates in Atlanta, Georgia: anthropogenic influences on biogenic  
586 secondary organic aerosol formation, *Atmos. Chem. Phys.*, 19, 3191-3206,  
587 10.5194/acp-19-3191-2019, 2019.
- 588 Hettiyadura, A. P. S., Stone, E. A., Kundu, S., Baker, Z., Geddes, E., Richards, K., and



- 589 Humphry, T.: Determination of atmospheric organosulfates using HILIC  
590 chromatography with MS detection, *Atmos. Meas. Tech.*, 8, 2347-2358,  
591 10.5194/amt-8-2347-2015, 2015.
- 592 Hettiyadura, A. P. S., Jayarathne, T., Baumann, K., Goldstein, A. H., de Gouw, J. A.,  
593 Koss, A., Keutsch, F. N., Skog, K., and Stone, E. A.: Qualitative and quantitative  
594 analysis of atmospheric organosulfates in Centreville, Alabama, *Atmos. Chem.*  
595 *Phys.*, 17, 1343-1359, 10.5194/acp-17-1343-2017, 2017.
- 596 Huang, L., Wang, Y., Zhao, Y., Hu, H., Yang, Y., Wang, Y., Yu, J. Z., Chen, T., Cheng,  
597 Z., Li, C., Li, Z., and Xiao, H.: Biogenic and Anthropogenic Contributions to  
598 Atmospheric Organosulfates in a Typical Megacity in Eastern China, *J. Geophys.*  
599 *Res. Atmos.*, 128, 10.1029/2023jd038848, 2023.
- 600 Jiang, H., Cai, J., Feng, X., Chen, Y., Wang, L., Jiang, B., Liao, Y., Li, J., Zhang, G.,  
601 Mu, Y., and Chen, J.: Aqueous-Phase Reactions of Anthropogenic Emissions  
602 Lead to the High Chemodiversity of Atmospheric Nitrogen-Containing  
603 Compounds during the Haze Event, *Environ. Sci. Technol.*, 57, 16500-16511,  
604 10.1021/acs.est.3c06648, 2023.
- 605 Kanellopoulos, P. G., Kotsaki, S. P., Chrysochou, E., Koukoulakis, K., Zacharopoulos,  
606 N., Philippopoulos, A., and Bakeas, E.: PM<sub>2.5</sub>-bound organosulfates in two  
607 Eastern Mediterranean cities: The dominance of isoprene organosulfates,  
608 *Chemosphere*, 297, 10.1016/j.chemosphere.2022.134103, 2022.
- 609 Kristensen, K., Bilde, M., Aalto, P. P., Petäjä, T., and Glasius, M.: Denuder/filter  
610 sampling of organic acids and organosulfates at urban and boreal forest sites:



- 611 Gas/particle distribution and possible sampling artifacts, *Atmos. Environ.*, 130,  
612 36-53, 10.1016/j.atmosenv.2015.10.046, 2016.
- 613 Li, J., Wang, G., Wu, C., Cao, C., Ren, Y., Wang, J., Li, J., Cao, J., Zeng, L., and Zhu,  
614 T.: Characterization of isoprene-derived secondary organic aerosols at a rural site  
615 in North China Plain with implications for anthropogenic pollution effects,  
616 *Scientific Reports*, 8, 10.1038/s41598-017-18983-7, 2018.
- 617 Li, L., Yang, W., Xie, S., and Wu, Y.: Estimations and uncertainty of biogenic volatile  
618 organic compound emission inventory in China for 2008–2018, *Sci. Total  
619 Environ.*, 733, 10.1016/j.scitotenv.2020.139301, 2020.
- 620 Li, L. Y. and Xie, S. D.: Historical variations of biogenic volatile organic compound  
621 emission inventories in China, 1981–2003, *Atmos. Environ.*, 95, 185-196,  
622 10.1016/j.atmosenv.2014.06.033, 2014.
- 623 Lin, X., Xu, Y., Zhu, R. G., Xiao, H. W., and Xiao, H. Y.: Proteinaceous Matter in  
624 PM<sub>2.5</sub> in Suburban Guiyang, Southwestern China: Decreased Importance in  
625 Long-Range Transport and Atmospheric Degradation, *J. Geophys. Res. Atmos.*,  
626 128, 10.1029/2023jd038516, 2023.
- 627 Liu, T., Xu, Y., Sun, Q. B., Xiao, H. W., Zhu, R. G., Li, C. X., Li, Z. Y., Zhang, K. Q.,  
628 Sun, C. X., and Xiao, H. Y.: Characteristics, Origins, and Atmospheric Processes  
629 of Amines in Fine Aerosol Particles in Winter in China, *J. Geophys. Res. Atmos.*,  
630 128, 10.1029/2023jd038974, 2023.
- 631 Lukács, H., Gelencsér, A., Hoffer, A., Kiss, G., Horváth, K., and Hartyáni, Z.:  
632 Quantitative assessment of organosulfates in size-segregated rural fine aerosol,



- 633 Atmos. Chem. Phys., 9, 231-238, 10.5194/acp-9-231-2009, 2009.
- 634 Ma, Q., Cai, S., Wang, S., Zhao, B., Martin, R. V., Brauer, M., Cohen, A., Jiang, J.,  
635 Zhou, W., Hao, J., Frostad, J., Forouzanfar, M. H., and Burnett, R. T.: Impacts of  
636 coal burning on ambient PM<sub>2.5</sub> pollution in China, Atmos. Chem. Phys., 17,  
637 4477-4491, 10.5194/acp-17-4477-2017, 2017.
- 638 Mason, S. A., Field, R. J., Yokelson, R. J., Kochivar, M. A., Tinsley, M. R., Ward, D.  
639 E., and Hao, W. M.: Complex effects arising in smoke plume simulations due to  
640 inclusion of direct emissions of oxygenated organic species from biomass  
641 combustion, J. Geophys. Res. Atmos., 106, 12527-12539,  
642 10.1029/2001jd900003, 2001.
- 643 Nozière, B., Ekström, S., Alsberg, T., and Holmström, S.: Radical-initiated formation  
644 of organosulfates and surfactants in atmospheric aerosols, Geophys. Res. Lett.,  
645 37, n/a-n/a, 10.1029/2009gl041683, 2010.
- 646 Riva, M., Tomaz, S., Cui, T., Lin, Y.-H., Perraudin, E., Gold, A., Stone, E. A.,  
647 Villenave, E., and Surratt, J. D.: Evidence for an Unrecognized Secondary  
648 Anthropogenic Source of Organosulfates and Sulfonates: Gas-Phase Oxidation  
649 of Polycyclic Aromatic Hydrocarbons in the Presence of Sulfate Aerosol,  
650 Environ. Sci. Technol., 49, 6654-6664, 10.1021/acs.est.5b00836, 2015.
- 651 Riva, M., Chen, Y., Zhang, Y., Lei, Z., Olson, N. E., Boyer, H. C., Narayan, S., Yee, L.  
652 D., Green, H. S., Cui, T., Zhang, Z., Baumann, K., Fort, M., Edgerton, E.,  
653 Budisulistiorini, S. H., Rose, C. A., Ribeiro, I. O., e Oliveira, R. L., dos  
654 Santos, E. O., Machado, C. M. D., Szopa, S., Zhao, Y., Alves, E. G., de Sá, S. S.,





655 Hu, W., Knipping, E. M., Shaw, S. L., Duvoisin Junior, S., de Souza, R. A. F.,  
656 Palm, B. B., Jimenez, J.-L., Glasius, M., Goldstein, A. H., Pye, H. O. T., Gold,  
657 A., Turpin, B. J., Vizuete, W., Martin, S. T., Thornton, J. A., Dutcher, C. S., Ault,  
658 A. P., and Surratt, J. D.: Increasing Isoprene Epoxydiol-to-Inorganic Sulfate  
659 Aerosol Ratio Results in Extensive Conversion of Inorganic Sulfate to  
660 Organosulfur Forms: Implications for Aerosol Physicochemical Properties,  
661 *Environ. Sci. Technol.*, 53, 8682-8694, 10.1021/acs.est.9b01019, 2019.

662 Schindelka, J., Iinuma, Y., Hoffmann, D., and Herrmann, H.: Sulfate radical-initiated  
663 formation of isoprene-derived organosulfates in atmospheric aerosols, *Faraday*  
664 *Discuss.*, 165, 10.1039/c3fd00042g, 2013.

665 Simpson, I. J., Akagi, S. K., Barletta, B., Blake, N. J., Choi, Y., Diskin, G. S., Fried,  
666 A., Fuelberg, H. E., Meinardi, S., Rowland, F. S., Vay, S. A., Weinheimer, A. J.,  
667 Wennberg, P. O., Wiebring, P., Wisthaler, A., Yang, M., Yokelson, R. J., and  
668 Blake, D. R.: Boreal forest fire emissions in fresh Canadian smoke plumes: C1-  
669 C10 volatile organic compounds (VOCs), CO<sub>2</sub>, CO, NO<sub>2</sub>, NO, HCN and  
670 CH<sub>3</sub>CN, *Atmos. Chem. Phys.*, 11, 6445-6463, 10.5194/acp-11-6445-2011, 2011.

671 Song, J., Li, M., Jiang, B., Wei, S., Fan, X., and Peng, P. a.: Molecular  
672 Characterization of Water-Soluble Humic like Substances in Smoke Particles  
673 Emitted from Combustion of Biomass Materials and Coal Using Ultrahigh-  
674 Resolution Electrospray Ionization Fourier Transform Ion Cyclotron Resonance  
675 Mass Spectrometry, *Environ. Sci. Technol.*, 52, 2575-2585,  
676 10.1021/acs.est.7b06126, 2018.



- 677 Song, J., Li, M., Fan, X., Zou, C., Zhu, M., Jiang, B., Yu, Z., Jia, W., Liao, Y., and  
678 Peng, P. a.: Molecular Characterization of Water- and Methanol-Soluble Organic  
679 Compounds Emitted from Residential Coal Combustion Using Ultrahigh-  
680 Resolution Electrospray Ionization Fourier Transform Ion Cyclotron Resonance  
681 Mass Spectrometry, *Environ. Sci. Technol.*, 53, 13607-13617,  
682 10.1021/acs.est.9b04331, 2019.
- 683 Surratt, J. D., Kroll, J. H., Kleindienst, T. E., Edney, E. O., Claeys, M., Sorooshian,  
684 A., Ng, L., Offenberg, J. H., Lewandowski, M., Jaoui, M., Flagan, R. C., and  
685 Seinfeld, J. H.: Evidence for organosulfates in secondary organic aerosol.,  
686 *Environ. Sci. Technol.*, 41, 517-527, 2007.
- 687 Surratt, J. D., Gómez-González, Y., Chan, A. W., Vermeylen, R., Shahgholi, M.,  
688 Kleindienst, T. E., Edney, E. O., Offenberg, J. H., Lewandowski, M., Jaoui, M.,  
689 Maenhaut, M. W., Claeys, M., Flagan, R. C., and Seinfeld, J. H.: Organosulfate  
690 Formation in Biogenic Secondary Organic Aerosol, *The Journal of Physical*  
691 *Chemistry A*, 112, 8345-8378, 2008.
- 692 Tang, J., Li, J., Su, T., Han, Y., Mo, Y., Jiang, H., Cui, M., Jiang, B., Chen, Y., Tang,  
693 J., Song, J., Peng, P. a., and Zhang, G.: Molecular compositions and optical  
694 properties of dissolved brown carbon in biomass burning, coal combustion, and  
695 vehicle emission aerosols illuminated by excitation–emission matrix  
696 spectroscopy and Fourier transform ion cyclotron resonance mass spectrometry  
697 analysis, *Atmos. Chem. Phys.*, 20, 2513-2532, 10.5194/acp-20-2513-2020, 2020.
- 698 Tao, S., Lu, X., Levac, N., Bateman, A. P., Nguyen, T. B., Bones, D. L., Nizkorodov,



- 699 S. A., Laskin, J., Laskin, A., and Yang, X.: Molecular Characterization of  
700 Organosulfates in Organic Aerosols from Shanghai and Los Angeles Urban  
701 Areas by Nanospray-Desorption Electrospray Ionization High-Resolution Mass  
702 Spectrometry, *Environ. Sci. Technol.*, 48, 10993-11001, 10.1021/es5024674,  
703 2014.
- 704 Wach, P., Spólnik, G., Rudziński, K. J., Skotak, K., Claeys, M., Danikiewicz, W., and  
705 Szmigielski, R.: Radical oxidation of methyl vinyl ketone and methacrolein in  
706 aqueous droplets: Characterization of organosulfates and atmospheric  
707 implications, *Chemosphere*, 214, 1-9, 10.1016/j.chemosphere.2018.09.026, 2019.
- 708 Wang, K., Zhang, Y., Huang, R.-J., Wang, M., Ni, H., Kampf, C. J., Cheng, Y., Bilde,  
709 M., Glasius, M., and Hoffmann, T.: Molecular Characterization and Source  
710 Identification of Atmospheric Particulate Organosulfates Using Ultrahigh  
711 Resolution Mass Spectrometry, *Environ. Sci. Technol.*, 53, 6192-6202,  
712 10.1021/acs.est.9b02628, 2019.
- 713 Wang, Y., Ma, Y., Kuang, B., Lin, P., Liang, Y., Huang, C., and Yu, J. Z.: Abundance  
714 of organosulfates derived from biogenic volatile organic compounds: Seasonal  
715 and spatial contrasts at four sites in China, *Sci. Total Environ.*, 806,  
716 10.1016/j.scitotenv.2021.151275, 2022.
- 717 Wang, Y., Zhao, Y., Wang, Y., Yu, J.-Z., Shao, J., Liu, P., Zhu, W., Cheng, Z., Li, Z.,  
718 Yan, N., and Xiao, H.: Organosulfates in atmospheric aerosols in Shanghai,  
719 China: seasonal and interannual variability, origin, and formation mechanisms,  
720 *Atmos. Chem. Phys.*, 21, 2959-2980, 10.5194/acp-21-2959-2021, 2021.



- 721 Wang, Y., Hu, M., Wang, Y.-C., Li, X., Fang, X., Tang, R., Lu, S., Wu, Y., Guo, S.,  
722 Wu, Z., Hallquist, M., and Yu, J. Z.: Comparative Study of Particulate  
723 Organosulfates in Contrasting Atmospheric Environments: Field Evidence for  
724 the Significant Influence of Anthropogenic Sulfate and NO<sub>x</sub>, *Environmental*  
725 *Science & Technology Letters*, 7, 787-794, 10.1021/acs.estlett.0c00550, 2020.
- 726 Wang, Y., Hu, M., Lin, P., Guo, Q., Wu, Z., Li, M., Zeng, L., Song, Y., Zeng, L., Wu,  
727 Y., Guo, S., Huang, X., and He, L.: Molecular Characterization of Nitrogen-  
728 Containing Organic Compounds in Humic-like Substances Emitted from Straw  
729 Residue Burning, *Environ. Sci. Technol.*, 51, 5951-5961,  
730 10.1021/acs.est.7b00248, 2017.
- 731 Wang, Y., Zhang, Y., Li, W., Wu, G., Qi, Y., Li, S., Zhu, W., Yu, J. Z., Yu, X., Zhang,  
732 H.-H., Sun, J., Wang, W., Sheng, L., Yao, X., Gao, H., Huang, C., Ma, Y., and  
733 Zhou, Y.: Important Roles and Formation of Atmospheric Organosulfates in  
734 Marine Organic Aerosols: Influence of Phytoplankton Emissions and  
735 Anthropogenic Pollutants, *Environ. Sci. Technol.*, 57, 10284-10294,  
736 10.1021/acs.est.3c01422, 2023.
- 737 Wang, Y., Hu, M., Guo, S., Wang, Y., Zheng, J., Yang, Y., Zhu, W., Tang, R., Li, X.,  
738 Liu, Y., Le Breton, M., Du, Z., Shang, D., Wu, Y., Wu, Z., Song, Y., Lou, S.,  
739 Hallquist, M., and Yu, J.: The secondary formation of organosulfates under  
740 interactions between biogenic emissions and anthropogenic pollutants in summer  
741 in Beijing, *Atmos. Chem. Phys.*, 18, 10693-10713, 10.5194/acp-18-10693-2018,  
742 2018.



- 743 Xu, J., Shen, G., Fu, B., Han, Y., Suo, X., Chen, Z., Lai, Y., Li, J., Li, L., Han, L., Tao,  
744 S., and Li, B.: Emissions of Particulate and Previously Ignored Gaseous  
745 Phosphorus from Coal and Biomass Combustion in Household Stoves,  
746 Environmental Science & Technology Letters, 10, 1011-1016,  
747 10.1021/acs.estlett.3c00029, 2023a.
- 748 Xu, Y., Dong, X. N., Xiao, H. Y., Zhou, J. X., and Wu, D. S.: Proteinaceous Matter  
749 and Liquid Water in Fine Aerosols in Nanchang, Eastern China: Seasonal  
750 Variations, Sources, and Potential Connections, J. Geophys. Res.Atmos., 127,  
751 10.1029/2022jd036589, 2022.
- 752 Xu, Y., Dong, X.-N., He, C., Wu, D.-S., Xiao, H.-W., and Xiao, H.-Y.: Mist cannon  
753 trucks can exacerbate the formation of water-soluble organic aerosol and PM<sub>2.5</sub>  
754 pollution in the road environment, Atmos. Chem. Phys., 23, 6775-6788,  
755 10.5194/acp-23-6775-2023, 2023b.
- 756 Xu, Y., Lin, X., Sun, Q. B., Xiao, H. W., Xiao, H., and Xiao, H. Y.: Elaborating the  
757 Atmospheric Transformation of Combined and Free Amino Acids From the  
758 Perspective of Observational Studies, J. Geophys. Res.Atmos., 129,  
759 10.1029/2024jd040730, 2024a.
- 760 Xu, Y., Liu, T., Ma, Y.-J., Sun, Q.-B., Xiao, H.-W., Xiao, H., Xiao, H.-Y., and Liu, C.-  
761 Q.: Measurement report: Occurrence of aminiums in PM<sub>2.5</sub> during winter in  
762 China – aminium outbreak during polluted episodes and potential constraints,  
763 Atmos. Chem. Phys., 24, 10531-10542, 10.5194/acp-24-10531-2024, 2024b.
- 764 Xu, Y., Miyazaki, Y., Tachibana, E., Sato, K., Ramasamy, S., Mochizuki, T.,



- 765 Sadanaga, Y., Nakashima, Y., Sakamoto, Y., Matsuda, K., and Kajii, Y.: Aerosol  
766 Liquid Water Promotes the Formation of Water-Soluble Organic Nitrogen in  
767 Submicrometer Aerosols in a Suburban Forest, *Environ. Sci. Technol.*, 54, 1406-  
768 1414, 10.1021/acs.est.9b05849, 2020.
- 769 Yang, T., Xu, Y., Ma, Y.-J., Wang, Y.-C., Yu, J. Z., Sun, Q.-B., Xiao, H.-W., Xiao, H.-  
770 Y., and Liu, C.-Q.: Field Evidence for Constraints of Nearly Dry and Weakly  
771 Acidic Aerosol Conditions on the Formation of Organosulfates, *Environmental  
772 Science & Technology Letters*, 10.1021/acs.estlett.4c00522, 2024.
- 773 Yang, T., Xu, Y., Ye, Q., Ma, Y.-J., Wang, Y.-C., Yu, J.-Z., Duan, Y.-S., Li, C.-X.,  
774 Xiao, H.-W., Li, Z.-Y., Zhao, Y., and Xiao, H.-Y.: Spatial and diurnal variations  
775 of aerosol organosulfates in summertime Shanghai, China: potential influence of  
776 photochemical processes and anthropogenic sulfate pollution, *Atmos. Chem.  
777 Phys.*, 23, 13433-13450, 10.5194/acp-23-13433-2023, 2023.
- 778 Yang, Y. R., Liu, X. G., Qu, Y., An, J. L., Jiang, R., Zhang, Y. H., Sun, Y. L., Wu, Z. J.,  
779 Zhang, F., Xu, W. Q., and Ma, Q. X.: Characteristics and formation mechanism  
780 of continuous hazes in China: a case study during the autumn of 2014 in the  
781 North China Plain, *Atmos. Chem. Phys.*, 15, 8165-8178, 10.5194/acp-15-8165-  
782 2015, 2015.
- 783 Yu, Q., Ding, X., He, Q., Yang, W., Zhu, M., Li, S., Zhang, R., Shen, R., Zhang, Y.,  
784 Bi, X., Wang, Y., Peng, P. a., and Wang, X.: Nationwide increase of polycyclic  
785 aromatic hydrocarbons in ultrafine particles during winter over China revealed  
786 by size-segregated measurements, *Atmos. Chem. Phys.*, 20, 14581-14595,



- 787           10.5194/acp-20-14581-2020, 2020.
- 788   Zhang, L., Li, J., Li, Y., Liu, X., Luo, Z., Shen, G., and Tao, S.: Comparison of  
789           water-soluble and water-insoluble organic compositions attributing to different  
790           light absorption efficiency between residential coal and biomass burning  
791           emissions *Atmos. Chem. Phys.*, 24, 6323-6337, 10.5194/acp-24-6323-2024,  
792           2024.
- 793   Zhang, L., Hu, B., Liu, X., Luo, Z., Xing, R., Li, Y., Xiong, R., Li, G., Cheng, H., Lu,  
794           Q., Shen, G., and Tao, S.: Variabilities in Primary N-Containing Aromatic  
795           Compound Emissions from Residential Solid Fuel Combustion and Implications  
796           for Source Tracers, *Environ. Sci. Technol.*, 56, 13622-13633,  
797           10.1021/acs.est.2c03000, 2022.
- 798   Zhang, Y., Zhang, R., Yu, J., Zhang, Z., Yang, W., Zhang, H., Lyu, S., Wang, Y., Dai,  
799           W., Wang, Y., and Wang, X.: Isoprene Mixing Ratios Measured at Twenty Sites  
800           in China During 2012–2014: Comparison With Model Simulation, *J. Geophys.*  
801           *Res. Atmos.*, 125, 10.1029/2020jd033523, 2020.
- 802   Zhou, Y., Xing, X., Lang, J., Chen, D., Cheng, S., Wei, L., Wei, X., and Liu, C.: A  
803           comprehensive biomass burning emission inventory with high spatial and  
804           temporal resolution in China, *Atmos. Chem. Phys.*, 17, 2839-2864, 10.5194/acp-  
805           17-2839-2017, 2017.
- 806   Zhu, Y., Yang, L., Chen, J., Wang, X., Xue, L., Sui, X., Wen, L., Xu, C., Yao, L.,  
807           Zhang, J., Shao, M., Lu, S., and Wang, W.: Characteristics of ambient volatile  
808           organic compounds and the influence of biomass burning at a rural site in



809 Northern China during summer 2013, Atmos. Environ., 124, 156-165,  
810 10.1016/j.atmosenv.2015.08.097, 2016.  
811